Applied Catalysis B: Environmental 94 (2010) 192–199

Contents lists available at ScienceDirect

Applied Catalysis B: Environmental

journal homepage: www.elsevier.com/locate/apcatb

Kinetics and initial photocatalytic pathway of tryptophan, important constituent of microorganisms

L. Elsellami [a,b], F. Vocanson [c,d], F. Dappozze [a], R. Baudot [e], G. Febvay [f], M. Rey [f], A. Houas [b], C. Guillard [a,*]

[a] Université Lyon1, CNRS, UMR 5256, IRCELYON, Institut de Recherches sur la Catalyse et l'Environnement de Lyon, 2 Avenue Albert Einstein, F-69626 Villeurbanne cedex, France
[b] Laboratoire de Catalyse et Environnement, Faculté des Sciences de Gabès, Tunisia
[c] Université de Saint-Etienne, F-42000 Saint-Etienne, France
[d] Laboratoire Hubert Curien, UMR 5516, F-42000 Saint-Etienne, France
[e] Service Central d'analyse du CNRS, Echangeur de Solaize B.P. 22, 69390 Vernaison, France
[f] INRA/INSA 203, Biologie Fonctionnelle, Insectes et Interactions BF2I, Villeurbanne, France

ARTICLE INFO

Article history:
Received 27 August 2009
Received in revised form 5 November 2009
Accepted 7 November 2009
Available online 13 November 2009

Keywords:
Photocatalysis
Amino acids
Tryptophan
Chemical pathways
Intermediates

ABSTRACT

The adsorption equilibrium in the dark and under UV light, the kinetic of photocatalytic oxidation and the main initial pathways of tryptophan photocatalytic degradation has been investigated in aerated TiO_2 Degussa P-25 aqueous suspensions illuminated at $\lambda > 340$ nm. Tryptophan has been chosen as a model of organic compounds of amino acids, elemental constituents of DNA, microorganisms, e.g. bacteria, fungi, virus among others to better understand their photocatalytic degradation.

Langmuir and Langmuir–Hinshelwood models have been used to determine the adsorption, the rate constants and the surface coverage of TiO_2. Despite a low coverage of the TiO_2 surface in the dark a high photocatalytic degradability and initial mineralization occurred. However, the surface coverage of TiO_2 was about doubled under UV light suggesting the formation of active sites under irradiation.

LC–MS, LC–UV with or without derivatization analyses allowed us to identify, mono-, di- and tri-hydroxylated compounds, deamination of heterocycle, the formation of six organic acid, oxalic, oxamique, lactic, formic, acetic and propanoic acids and of three linear amino acids, serine, aspartic acid and glycine. A degradation mechanism is proposed to the formation of oxamic acid.

The study of the mineralization of carbon and nitrogen showed the presence of trace of organic molecules mineralizable with difficulty. Nitrogen atoms were predominantly photoconverted into NH_4^+. After more than 95% of carbon mineralization, NH_4^+/NO_3^- ratio was 4.

The identification of the photocatalytic products, their evolution and the TOC evolution indicated three initial competitive pathways: about 50% of hydroxylation with 6–7% of the hydroxylation of carbon bearing NH_2 and COO^-, about 30% of decarboxylation and less than 20% of nitrogen–carbon (N–C) cleavage.

1. Introduction

Recently, the increases interest in the effects of photocatalysis on living matter has simulated many investigations into the degradation of microorganisms. The application of TiO_2 in biological fields, such as antibacterial effects [1–8] and medical treatments for diseases, including cancer [9], has also been extensively progressive. However, the mechanism of degradation is not very well known and the intermediate products are less studied. Muszkat et al. [10,11] have analyzed the amount of amino acids in decomposed proteins and our previous work showed the presence of organic acid [8] in the photocatalytic degradation of *Escherichia coli*. However, due to the complexity of microorganism and protein, it is important to work on simpler systems of biochemical interest to assess the fate of the elemental constituents of such system. Of particular importance are the amino acids, which are the building blocks of proteins.

Moreover they are found behind filtration process [12,13] and are known to form odorous by-products after chlorination process [14].

Our objectives are to contribute to a better understanding of photocatalytic mechanism for removing amino acids, which are the simplest molecules constituting the microorganisms e.g. bacteria, fungi, virus, mold, among others (DNA, RNA, proteins, etc.) by studying the kinetics of adsorption in the dark and under UV, the kinetics of photocatalytic degradation at different concentrations and the fate of carbon and nitrogen atom.

Tryptophan has been chosen as a model of amino acids due to the presence of indole and benzenic cycle. Tryptophan is an

* Corresponding author. Tel.: +33 44 72 53 16; fax: +33 4 72 44 53 99.
E-mail address: chantal.guillard@ircelyon.univ-lyon1.fr (C. Guillard).

0926-3373/$ – see front matter © 2009 Elsevier B.V. All rights reserved.
doi:10.1016/j.apcatb.2009.11.009

essential amino acid for our life. Proteins contain about 1% of this amino acid.

Attention is focused on the determination of degradation pathways by means of the determination of initial rate and of the identification and quantification of intermediate product of photocatalytic degradation by measuring TOC, the formation of NO_3^- and NH_4^+ and of aromatic and linear organic compounds.

2. Experimental

2.1. Photocatalyst

The photocatalyst used was TiO_2 Degussa P-25, which is made of anatase (80%) and rutile (20%) under the shape of non-porous particles with a surface area of 50 m^2/g and mean crystallite sizes of ca. 30 nm.

2.2. Adsorption tests

The adsorption isotherm of tryptophan on TiO_2 was determined in the dark by using 20 mL of aqueous solution of tryptophan of various initial concentrations and natural pH (pH = 6.4 ± 0.2). After 30 min of mechanical stirring, time necessary to reach the equilibrium, the aqueous samples were filtered through 0.45 μm millipores discs to remove TiO_2 powder before analysing.

2.3. Photocatalytic degradation

Experiments were carried out in a Pyrex cylindrical flask, opened to air with an optical window of 19 cm^2 area. The volume of the solution was 20 mL. For these experiments, TiO_2 slurry concentration was set at 1.25 g/L, in order to absorb all the photons [15]. The light source was a HPK 125 W Philips mercury lamp, cooled with a water circulation. The irradiation spectrum was cut-off below 340 nm using a Corning 0.52 filter. The radiant flux was measured using a radiometer (United Detector Technology Inc., Model 21A power meter). It has been found that the number of absorbed photons by TiO_2 in the irradiated cell was about 1.3×10^{17} photons per second.

2.4. Analysis

Amino acid analysis was done by HPLC (Agilent 1100; Agilent Technologies, Massy, France) with a guard cartridge and a reverse phase C18 column (Zorbax Eclipse-AAA 3.5 μm, 150 mm × 4.6 mm, Agilent Technologies). Prior to injection, the sample was buffered with borate at pH 10.2, and primary amino acids were derivatized with o-phthalaldehyde (OPA) using 3-mercaptopropionic acid (3-MPA). The secondary amino acids, which did not react with the OPA, were then derivatized with 9-fluorenylmethyl chloroformate (FMOC). The derivatization process at room temperature was automated using the Agilent 1313A autosampler as described below. Initially 2.5 μL of borate buffer (0.4 M, pH 10.2) was mixed with 0.5 μL of sample. Derivatization was done by adding and mixing successively 0.5 μL of 10 mg/mL OPA reagent dissolved in 0.4 M borate buffer and 3-MPA, and 0.5 μL of 2.5 mg/mL FMOC reagent dissolved in acetonitrile. Finally the mixture was diluted with 32 μL H_2O. Between each of the above pipetting steps there was a needle wash using water or acetonitrile. A total volume of 18 μL was then injected onto the column. Separation was carried out at 40 °C with a flow rate of 2 mL/min using 40 mM Na_2HPO_4 (eluent A, pH 7.8, adjusted with NaOH) as polar phase and an acetonitrile/methanol/water mixture (45/45/10, v/v/v) as nonpolar phase (eluent B). The following gradient was applied: start 0% B, 1.9 min 0% B, 18.1 min 57% B, 18.6 min 100% B, 22.3 min 100% B, and 23.2 min 0% B for equilibration. Detection was performed by a UV diode array detector at 338 nm for the primary amino acids (OPA-derivatized) and at 262 nm for the secondary amino acids (FMOC-derivatized). For quantification norvaline was used as internal standard and response factor of each amino acid was determined using a 250 pmol/μL standard mixture of 21 amino acids. The limit of quantification of amino acid is about 0.1 μmol/L. Linear amino acid is concentrated by evaporation under vacuum.

The HPLC–MS identification of photoproducts was performed with a Hewlett-Packard HP 1100 series LC–MSD using a column Hypersyl BDS C18 (125 mm × 4 mm, particle size 5 μm). Isocratic elution conditions were applied. The mobile phase composition was H_2O buffered at pH = 5 with CH_3–COO–NH_4/acetonitrile at a ratio of 5/95. The flow rate was 0.3 mL/min and the injection volume was equal to 20 μL. The MS detection was carried out with electrospray ionization (ESI) in positive. The parameters of nebulization were the following: capillary potential = 4000 V, auxiliary gas = N_2, flow rate = 12 L/min, and pressure = 55 psig.

The formation of carboxylic acids has been analyzed by LC using a Waters 600 pump, a Waters 486 UV detector (detection at 210 nm), and a Sarasep CAR-H (300 mm × 4.6 mm) column. The flow rate was 0.7 mL/min. The injection volume was 100 μL and the mobile phase was H_2SO_4 5×10^{-3} mol/L.

The formation of nitrate ions has been followed using ionic chromatography with a Dionex DX-120 pump and conductivity detector, and an IonPac AS14A (250 mm × 4 mm) column. The flow rate was 1 mL/min and the mobile phase was an alkaline buffer ($NaHCO_3$ 1.0 mmol/L + Na_2CO_3 8.0 mmol/L).

The formation of ammonium ions has also been followed using ionic chromatography with a Dionex DX-120 pump and conductivity detector. In this case a CS 12A (250 mm × 4 mm) column. The flow rate was 1 mL/min and the mobile phase was H_2SO_4 solutions containing 610 μL of pure sulfuric acid.

3. Results

3.1. Adsorption

The amount of tryptophan (Tryp) adsorbed per gram of TiO_2 reported as a function of the Tryp concentration present in solution (C_{eq}) was represented in Fig. 1.

Whatever the initial concentration of tryptophan, the amount adsorbed at equilibrium corresponds to less than 1% of OH covered by considering that adsorption of Tryp occurs on OH group present on the TiO_2 solid surface, which represent about 5 OH/nm^2 [16]. This amount corresponds to an areal density of adsorbed Tryp of 0.07 molecules/nm^2.

This low coverage of OH could partially be explained taking into account the work of Tran et al. [17], which suggest that effective adsorption for tryptophan should be only on basic terminal OH on the solid surface.

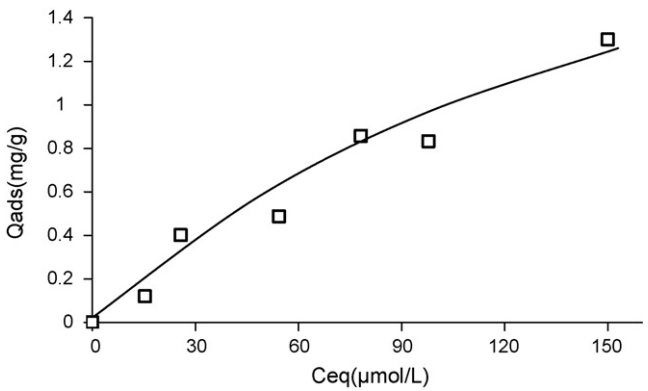

Fig. 1. Amount of tryptophan adsorbed per gram of catalyst.

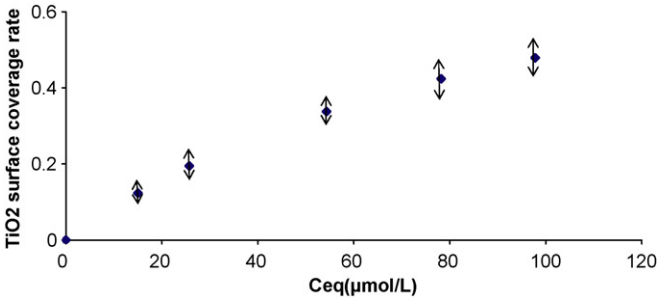

Fig. 2. Coverage rate as a function of Tryp concentration remaining in solution at the equilibrium.

On the contrary of phenylalanine adsorption, which seems to occur in multilayer [18], in the case of Tryp, the Tryp adsorption equilibrium can be modelized by Langmuir equation.

From Fig. 1, adsorption constant (K_{ads}) and the maximal adsorbed quantity of Tryp (Q_{max}) can be determined by the method of the least squares fitting according to the following equation:

$$\frac{Q_{ads}}{Q_{max}} = \frac{K_{ads}C_{eq}}{1 + K_{ads}C_{eq}}$$

where Q_{ads} is the adsorbed quantity of tryptophan and C_{eq} is the concentration of the compound at the adsorption equilibrium. Taken into account the values of $Q_{max} = 1.5 \pm 0.3$ mg/g and K_{ads} (dark) = 0.009 ± 0.003 L/µmol. The coverage rate $\theta = Q_{ads}/Q_{max}$, reported Fig. 2 indicates that about $46 \pm 8\%$ of TiO_2 surface is covered at a concentration of 100 µmol/L.

3.2. Kinetics and quantum yields

The disappearances of five different initial concentrations of Tryp are reported in Fig. 3 by plotting the evolution of the Tryptophan concentration as a function of irradiation time. The time necessary to observe a complete disappearance of tryptophan increases with Tryp concentration, it is within 8, 15, 25, 35 and 45 min for initial concentration of 18, 25, 58, 82 and 102 µmol/L, respectively in the presence of 1.25 g/L of TiO_2 and a pH of 6.5. The direct photolysis at $\lambda > 340$ nm was negligible indicating that disappearance observed in the presence of TiO_2 and UV at this wavelength is only due to photocatalytic process.

The variation of the pH during the degradation is negligible due to the important formation of ammonium ions, which consume proton released during the formation of organic acid.

The initial disappearance rate of Tryp represented as a function of the concentration of Tryp remaining in solution (C_{eq}) (Fig. 4)

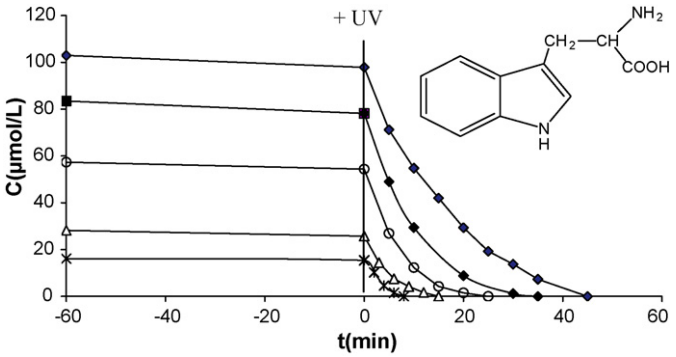

Fig. 3. Kinetics of tryptophan diasappearance for different initial concentrations.

reveals that below 25 µmol/L the initial rate is proportional to the Tryp concentration in solution ($r = kKC_{eq}$ with kK equal to 0.14 min^{-1}) and then reach a plateau. This type of curve can be modelized from a Langmuir–Hinshelwood model, $r = kKC_{eq}/1 + KC_{eq}$ where r is the initial rate of Tryp disappearance, k rate constant, K adsorption constant and C_{eq} the concentration of Tryp remaining in solution at equilibrium.

From Fig. 4 the rate constant k and the adsorption constant K can be extracted and the surface coverage ($\theta = KC/1 + KC$) under UV can be determined. The values of k and K are 6.7 µmol/L/min and 0.044 L/µmol, respectively. Surface coverage under UV is represented in Fig. 5. More than 80% of TiO_2 surface coverage was observed as early as a concentration of 60 µmol/L, whereas in the phenylalanine photocatalytic degradation the surface coverage was only 50% for a concentration of 240 µmol/L [18]. This result is in agreement with different types of adsorption of these both amino acids. As suggested by Horikoshi et al. [19] phenylalanine will be mainly adsorbed by NH_2 present on linear chain, whereas nitrogen of heterocycle of tryptophan will be strongly in interaction with OH terminal in the case of tryptophan [17]. In other words we can suggest that phenylalanine will be adsorbed vertically or tilted with a smaller angle to the normal of the TiO_2 surface, whereas tryptophan could be nearly adsorbed flat on TiO_2 surface in the dark.

The quantum yield, $\rho = 0.9\%$ observed for tryptophan (Eqs. (1) and (2)) at a concentration of 60 µmol/L is similar to this one observed obtained for phenylalanine [18]; however, in the case of tryptophan this quantum yield does not increase above this value whereas it reached 1.6% for phenylalanine.

$$\rho = \frac{r}{\varphi_n} \quad (1)$$

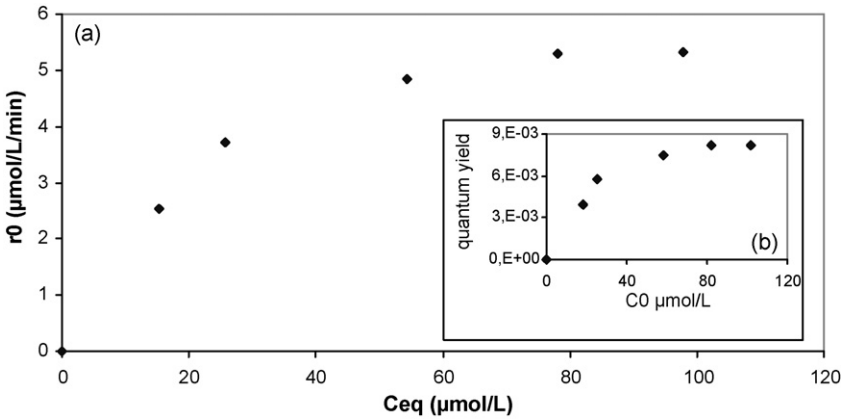

Fig. 4. (a) Evolution of initial rate of disappearance of tryptophan. In insert (b) is represented the evolution of quantum yield as a function of the concentration of remaining in solution (C_{eq}).

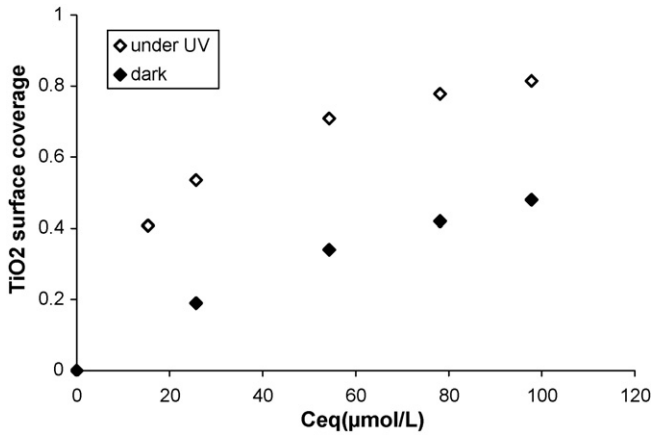

Fig. 5. Evolution of surface coverage as a function of tryptophan equilibrium concentration in the dark and under UV.

$$\varphi_n = \frac{(\Phi/E) \times S}{N_A} \quad (2)$$

with the radiant flux Φ in W cm^{-2} (J s^{-1} cm^{-2}), the radiant flux energy E in J Photons^{-1}, N_A the Avogadro's number and S the surface of optical window.

From Fig. 5 it is interesting to notice that surface coverage is not similar considering dark adsorption or UV adsorption. Adsorption constant is 0.0094 L/μmol in the dark whereas it is 0.044 L/μmol under UV-irradiation.

This behaviour has already been observed in our laboratory [20], and by several other authors [21–31].

Several hypotheses have already been suggested to explain this phenomenon.

- The reaction takes place not only on the surface but also near the surface.
- The active sites can be modified under UV-light considering:
  - The variation of the electronic properties of the TiO_2 surface under UV-irradiation and under UV ($Ti^{4+} \rightarrow Ti^{3+}$; $O^{2-} \rightarrow O^{\circ-}$).
  - The recombination reactions of active species (electron/hole or radical) occurring during the irradiation process can modify the thermodynamic equilibrium at the semiconductor surface due to the heat generated during the recombination as described below: $h\nu + TiO_2 \rightarrow e^-_{CB} + h^+_{VB} \rightarrow$ heat

3.3. Mineralization

Total mineralization is the ultimate step of the photocatalytic degradation of organic molecules. In order to quantify this process, Total Organic Carbon (TOC) and the evolution of nitrate and ammonium ions are followed as a function of time.

The disappearances of TOC (TOC measured) and of organic carbon issue from tryptophan remaining in solution (OC tryptophan) are represented in Fig. 6. Difference of these both curves corresponds to all organic carbons non-mineralised.

TOC disappeared from the beginning of irradiation indicating initial decarboxylation reaction. By comparing the initial evolution of TOC and tryptophan, about 30% of decarboxylation initially occurs.

After complete elimination of Tryp (50 min), only about 60% of the value of TOC expected from total mineralization was obtained and 2 h is necessary to mineralize about 95% of carbon.

The evolution profiles for NO_3^- and NH_4^+ are presented in Fig. 7. NH_4^+ ions appear from the beginning of the degradation and are

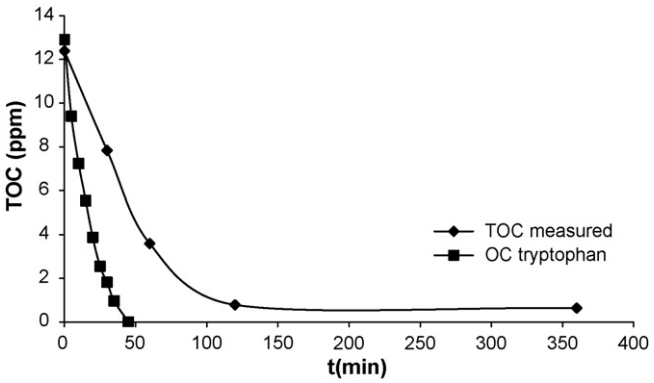

Fig. 6. Evolution of Total Organic Carbon in the degradation of 98 μmol/L of tryptophan.

the major one. The formation of nitrates occurred only after the total disappearance of tryptophan (about 1 h) indicating that nitrate ions are not primary oxidation by-products and come from intermediate compounds. After an irradiation time of 8 h, more than 95% of nitrogen initially present in Tryp was converted into ammonium and nitrate ions, about 80% and 20%, respectively.

The formation rate of NH_4^+ is about 5-fold lower than the rate of tryptophan degradation suggesting that deamination is not the major step of photocatalytic degradation. The selectivity expressed as $[NH_4^+]/2(C_0 - C_t)]$ is about 20% after 5 min for a conversion of 30% of Tryp.

The more important formation of NH_4^+ ions is in agreement not only with the work of Hidaka and co-workers on different amino acids [32] but also with our previous work showing that amine group is mainly transformed into ammonium in the beginning of reaction [33]. Actually, oxidation degree of amine group and ammonium is equal to +3. The formation of ammonium can be explained considering the reaction of e^- on protonated amine (Eq. (3)) as suggested by Möning et al. [34]. Actually in our pH conditions (pH = 6.5) more than 99% of tryptophan is present under amphoter structure.

(3)

3.4. Intermediates

3.4.1. Aromatic intermediates

The difference between tryptophan disappearance and its mineralization reflects the presence of several intermediate

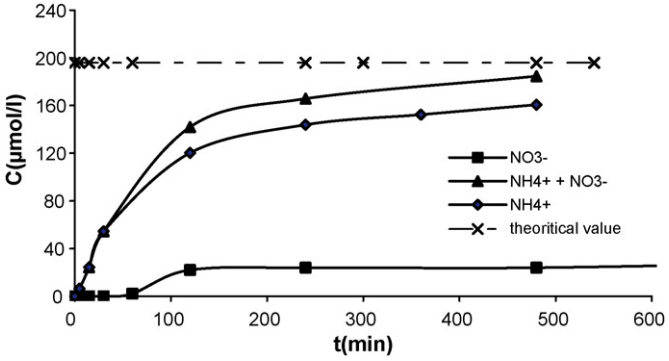

Fig. 7. Evolution of nitrate and ammonium ions in the degradation of 98 μmol/L of tryptophan.

Table 1
Possible chemical structure for photocatalytic products detected by LC–ESI-MS.

ESI^+ $m/z = M+1$	Molecular weight	Retention time (min)	Position	Structure
237	236	5.39	+2OH	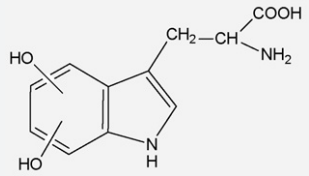
221	220	5.86	+OH	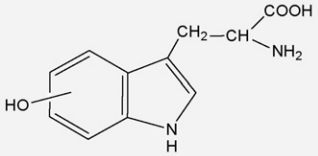
253	252	6.52	+3OH	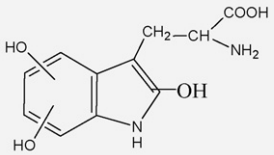
174	173	6.94	$-NH_2$ $-OH$	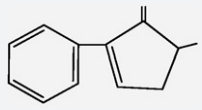
192	191	7.77	$-NH_2$	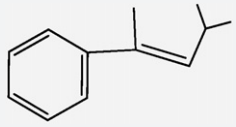
237	236	9.06	+2OH	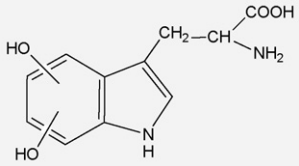
221	220	9.74	+OH	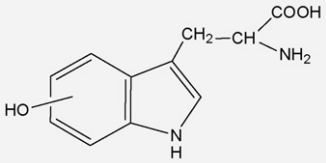

compounds during its oxidation. The reaction was stopped at 20 min for analysing the samples. This irradiation time has been chosen because the number of peaks and their intensities observed on HPLC/UV chromatogram are the most important.

Main intermediate products detected by LC–MS are listed in Table 1.

These different structures correspond to the following reactions:

(i) Hydroxylation occurring on the aromatic ring (compounds at t_R = 5.86 min and t_R = 9.74 min).
(ii) Dihydroxylation (compounds at t_R = 5.39 min and t_R = 9.06 min).
(iii) Trihydroxylation (compounds at t_R = 6.52 min).
(iv) Deamination of heterocycle (compounds at t_R = 6.94 min and t_R = 7.77 min).

The evolution of mono-hydroxylated (at t_R = 5.86 min and t_R = 9.74 min) and di-hydroxylated compounds (t_R = 5.39 min and t_R = 9.06 min) has been monitored by LC–UV as a function of time and confirm that the products at t_R = 5.86 min and t_R = 9.74 min are primary compounds, whereas the products t_R = 5.39 min and t_R = 9.06 min are only formed when the mono-hydroxylated compounds begin to disappear.

Some works [35–39] deal with the influence of the substituent on the selective photocatalytic oxidation of aromatic compounds in aqueous TiO_2 suspensions. In the present case, nitrogen atom of triazinic cycle, electrodonor group, is present on benzenic cycle

and active ortho and para position of aromatic ring as indicated with arrows, considering an electrophilic attack:

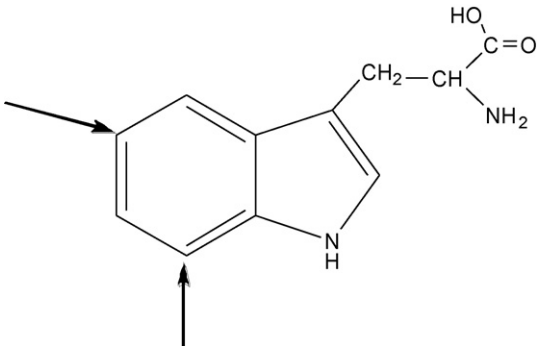

Accordingly, two positions on the aromatic cycle could be preferentially hydroxylated in agreement with the results obtained by LC/MS (peak t_R = 5.86 min and t_R = 9.74 min).

The detection of a tri-hydroxylated compound suggests that one of the hydroxylation is situated on heterocycle (peak t_R = 6.52 min).

The detection of compounds at t_R = 6.94 min and t_R = 7.77 min shows the deamination of heterocycle. Peak A has not been identified.

No decarboxylation compound has been evidenced, whereas the decarboxylation seems to be important regarding the evolution of TOC. The absence of decarboxylation products could be explained considering that amine intermediates formed could have important interaction with residual OH of the C18 column and not be eluted in our experimental conditions.

3.4.2. Carboxylic acids

The evolution of oxalic, oxamique, lactic, formic, acetic and propanoic acids was followed during the photocatalytic degradation (Fig. 8). Oxamic acid (NH_2–CO–COOH), containing a nitrogen atom and oxalic acid are the most important. The selectivity of oxamic acid is about 6–7% at 5 min of irradiation (30% of Tryp conversion). Abstraction of hydrogen by attack of OH radical on carbon bearing carboxylic and amino group and then addition of O_2 molecule can be suggested to explain the formation of oxamic acid considering the type of reaction proposed in the photocatalytic reactions [40] (Fig. 9).

Oxamic and oxalic acids appear from the beginning and increase until a maximum corresponding to the time necessary to the complete disappearance of tryptophan in solution. The four

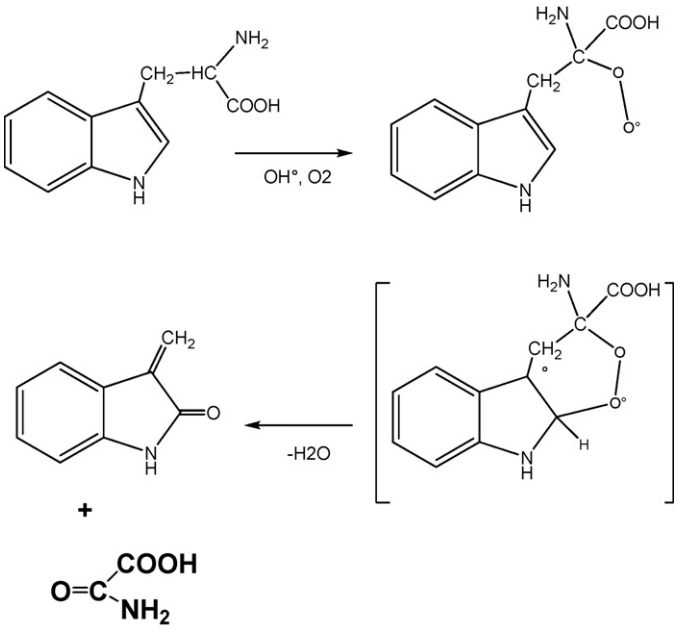

Fig. 9. Proposition of oxamic acid formation in the degradation of tryptophan.

other acid compounds are not primary products. The organic carbon coming from these different acids has been compared to the experimental TOC found in solution (Fig. 10). It is very interesting to notice that after total disappearance of tryptophan about 80% of organic matter provides from acid compounds.

Taking into account the concentration of NH_4^+, NO_3^- and oxamic acid, after total disappearance of Tryp about 35% of organic nitrogen compounds are not identified ([NH_4^+] = 100 μmol/L; [NO_3^-] = 0 μmol/L and [oxamic acid] = 28 μmol/L and less than 20% of organic nitrogen remains not identified after about 2 h of irradiation ([NH_4^+] = 122 μmol/L; [NO_3^-] = 25 μmol/L and [oxamic acid] = 18 μmol/L) while non-identified carbon seems very low (less than 10%).

After 6 h, organic matter containing carbon and nitrogen atom seems persisting in solution. However, taking into account the precision of measurement it is not possible to determine the number of carbon and nitrogen non-mineralised.

3.4.3. Linear amino acid formed

During the photocatalytic degradation of tryptophan we also identified traces of linear amino acids, serine, aspartic acid and

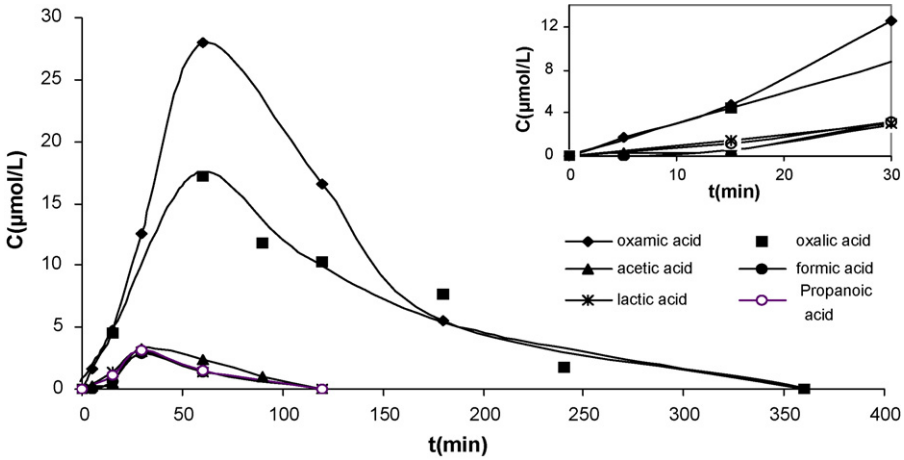

Fig. 8. Evolution of all carboxylic acids identified during the photocatalytic degradation of tryptophan ([Tryp] = 98 μmol/L).

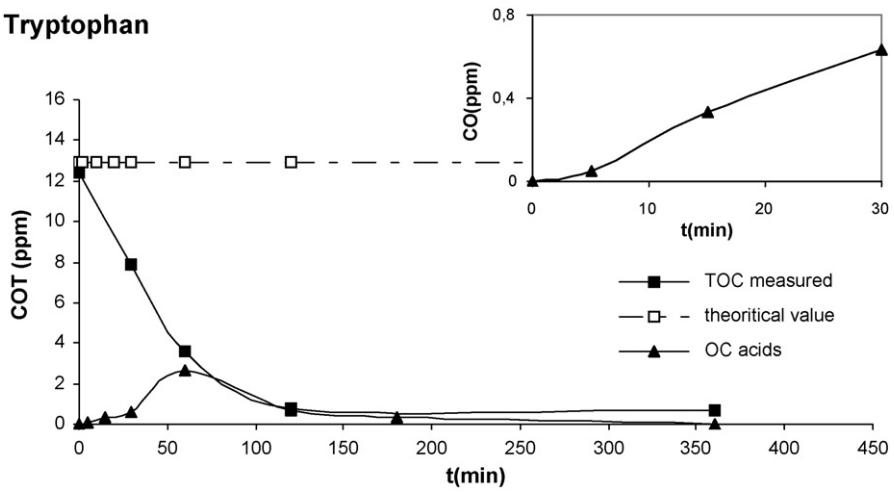

Fig. 10. Evolution of the ratio between organic carbon issue to carboxylic acids and TOC present in solution during the photocatalytic degradation of tryptophan ([Tryp] = 98 μmol/L).

Table 2
Linear amino acids identified after 40 min of photocatalytic degradation of a solution of 98 μmol/L of tryptophan.

Name	Formula	C (μmol/L)	C (μmol/L)/ C_{try} disappeared
Glycine	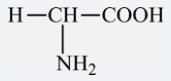	0.521	0.53%
Serine	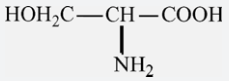	0.126	0.12%
Aspartic acid	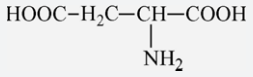	0.944	0.96%

glycine. Their quantification has been done only after 40 min of irradiation and after concentration (see Section 2).

Their structure, amount and selectivity are reported in Table 2.

Their presence shows that aliphatic chain can be broken either between CH and CH_2 to form glycine or between CH_2 and heterocycle to form serine. Considering the detection of aspartic acid, the break can also occur by rupture of heterocycle. This acid could be formed by oxidation of the double bond of peak F observed by LC/MS and proving of deamination of heterocycle.

4. Conclusions

The adsorption equilibrium and photocatalytic degradation of tryptophan in the presence of a suspension of TiO_2 Degussa P-25 have been modelized by Langmuir and Langmuir–Hinshelwood equation, respectively. Surface coverages of TiO_2, calculated using adsorption constant are totally different in the dark and under UV. It is about the double under UV suggesting either that these models are not applicable or that the active sites or their number is modified under UV light (under UV: $Ti^{4+} \rightarrow Ti^{3+}$ and $O^{2-} \rightarrow O^{\circ-}$). The quantum yield reaches a maximum value of 0.8%. The study of tryptophan mineralization by measuring Total Organic Carbon and the formation of ammonium and nitrate ions shows that 2 h of irradiation is necessary to mineralize more than 95% of carbon, whereas the total disappearance of tryptophan occurs before 50 min showing the formation of many intermediate products. Ammonium ions are detected from the beginning and are the major inorganic ions formed. Their formation is attributed to the transfer of electron to amine group, which is in our experimental condition positively charged.

Seven aromatic products were identified by LC–MS techniques corresponding to mono-, di- and tri-hydroxylated compounds and to deamination, six linear organic acid and three linear amino acids. The great number of compounds detected during the tryptophan degradation shows the complexity of the photocatalytic process and suggests the existence of various degradation routes resulting in multi-step and interconnected pathways. However, taking into account these different analysis we suggest that initially (for a conversion equal at about 30%), the disappearance of tryptophan is due to about 30% of decarboxylation products (calculated considering TOC), 20% of deazotation and 6–7% of hydroxylation of aliphatic chain, considering that hydroxylation of carbon bearing carboxylate and amino groups gives oxamic acid. The quantification of hydroxylated compounds on aromatic ring or on other atoms has not been quantified due to the absence of commercial products.

Acknowledgement

This work was supported by a CMCU Project "04PRE01".

References

[1] T. Matsunaga, R. Tomoda, Y. Nakajima, N. Nakamura, T. Komine, Appl. Environ. Microbiol. 54 (1988) 1330.
[2] K. Sunada, T. Watanabe, K. Hashimoto, Environ. Sci. Technol. 37 (2003) 4785.
[3] T. Saito, T. Iwase, T. Morioka, J. Photochem. Photobiol. B: Biol. 14 (1992) 369.
[4] P.C. Maness, S. Smolinski, D.M. Blake, Z. Huang, E.J. Wolfrum, W.A. Jacoby, Appl. Environ. Microbiol. 65 (1999) 4094.
[5] A.G. Rincon, C. Pulgarin, Appl. Catal. B: Environ. 49 (2004) 99.
[6] A.K. Benabbou, Z. Derriche, C. Felix, P. Lejeune, C. Guillard, Appl. Catal. B: Environ. 76 (2007) 257.
[7] C. Guillard, T.-H. Bui, C. Felix, V. Moules, B. Lina, P. Lejeune, C. R. Chim. 11 (2008) 107–113.
[8] T.-H. Bui, C. Felix, S. Pigeot-Remy, J.-M. Herrmann, P. Lejeune, C. Guillard, J. Adv. Oxid. Tech. 11 (3) (2008) 510.
[9] Y. Kubota, T. Shuin, C. Kawasaki, M. Hosaka, H. Kitamura, R. Cai, H. Sakai, K. Hashimoto, A. Fujishima, Br. J. Cancer 70 (1994) 1107.
[10] L. Muszkat, L. Feigelson, L. Bir, K.A. Muszkat, J. Photochem. Photobiol. B 60 (2001) 32.
[11] L. Muszkat, L. Feigelson, L. Bir, K.A. Muszkat, Pest. Manage. Sci. 58 (2002) 1143.
[12] K.M. Agbekodo, J.P. Croué, S. Dard, B. Legube, Revue des sciences de l'eau (Rev. Sci. Eau.) 4 (1996) 535.
[13] I.C. Escobar, S. Hong, A.A. Raudall, J. Membr. Sci. 175 (2000) 1.
[14] I. Freuze, S. Brosillon, D. Herman, A. Laplanche, C. Democrate, J. Cavard, Environ. Sci. Technol. 38 (2004) 4134.

[15] M. El Madani, C. Guillard, N. Pérol, J.M. Chovelon, M. El Azzouzi, A. Zrineh, J.M. Herrmann, Appl. Catal. B: Environ. 65 (2006) 70–76.
[16] H.P. Boehm, Adv. Catal. 16 (1966) 179.
[17] T.-H. Tran, A.Y. Nosaka, Y. Nasaka, J. Phys. Chem. B 110 (2006) 25525.
[18] L. Elsellami, F. Vocanson, E. Puzenat, A. Houas, C. Guillard, Water Res, submitted for publication.
[19] S. Horikoshi, N. Serpone, J. Zhao, H. Hidaka, J. Photochem. Photobiol. A: Chem. 118 (1998) 123.
[20] M. El Madani, C. Guillard, N. Pérol, J.M. Chovelon, M. El Azzouzi, A. Zrinet, J.M. Herrmann, Appl. Catal. B: Environ. 65 (2006) 70.
[21] S. Parra, J. Oliveiro, C. Pulgarin, Appl. Catal. B: Environ. 36 (2002) 75.
[22] J. Cunningham, S. Srijanarai, J. Photochem. Photobiol. A: Chem. 58 (1991) 361.
[23] A. Mills, S. Morris, J. Photochem. Photobiol. A: Chem. 71 (1993) 75.
[24] J. Cunningham, G.H. Al-Sayyed, J. Chem. Soc., Faraday Trans. 86 (1990) 3935.
[25] J. Cunningham, P. Sedlak, in: D.F. Ollis, I.I. Al-Ekabi (Eds.), Photocatalytic Purification and Treatment of Water and Air, Elsevier, Amsterdam, 1993.
[26] Y. Xu, C.H. Langford, J. Photochem. Photobiol. A: Chem. 133 (2000) 67.
[27] C. Minero, Sol. Energy Mater. Sol. Cells 38 (1995) 421.
[28] C. Minero, E. Pelizzetti, S. Malato, J. Blanco, Solar Energy 56 (1996) 411.
[29] C. Minero, Catal. Today 54 (1999) 205.
[30] A.V. Emeline, V. Ryabchuk, N. Serpone, J. Photochem. Photobiol. A 133 (2000) 89.
[31] S. Brosillon, L. Lhomme, C. Vallet, A. Bouzaza, D. Wolbert, Appl. Catal. B: Environ. 78 (2008) 232.
[32] H. Hidaka, S. Horikoshi, K. Ajisaka, J. Zhao, N. Serpone, J. Photochem. Photobiol. A: Chem. 108 (1997) 197–205.
[33] T.-H. Bui, M. Karkmaz, E. Puzenat, C. Guillard, J.-M. Herrmann, Res. Chem. Intermed. 33 (2007) 421.
[34] J. Möning, R. Chapman, K.-D. Asmus, J. Phys. Chem. 89 (1985) 3139.
[35] M. Brigante, C. Emmeli, C. Ferronato, M.-D. Greca, L. Previtera, J.-O. Paisse, J.-M. Chovelon, Chemosphere 68 (2007) 464.
[36] M. Mekkaoui, M. El Azzouzi, A. Bouhaouss, M. Ferhat, A. Dahchour, S. Guittonneau, Meallier, Fresenius Environ. Bull. 9 (2000) 783.
[37] J.C. Garcia, K. Takashima, J. Photochem. Photobiol. A: Chem. 155 (2003) 215.
[38] P. Pizarro, C. Guillard, N. Perol, J.M. Herrmann, Catal. Today 101 (2005) 211.
[39] C. Bliefert, R. Perraud, Chimie de l'Environnement Air, Eau, Sols, Déchets, Deboeck Université, 2001„ p. 291.
[40] L. Cermenati, P. Pichat, C. Guillard, A. Albini, J. Phys. Chem. 2650 (1997) 101.